Reduced Voltage Sensitivity of Activation of P/Q-Type Ca^{2+} Channels is Associated with the Ataxic Mouse Mutation *Rolling Nagoya* (tg^{rol})

Yasuo Mori,[1,2] Minoru Wakamori,[1] Sen-ichi Oda,[3] Colin F. Fletcher,[4] Naomi Sekiguchi,[1] Emiko Mori,[1] Neal G. Copeland,[4] Nancy A. Jenkins,[4] Kaori Matsushita,[1,2] Zenjiro Matsuyama,[1] and Keiji Imoto[1,2]

[1]Department of Information Physiology, National Institute for Physiological Sciences, and [2]School of Life Science, The Graduate University for Advanced Studies, Okazaki, Aichi 444–8585, Japan, [3]Laboratory of Animal Management, School of Agricultural Sciences, Nagoya University, Nagoya, Aichi 464–8601, Japan, and [4]Mammalian Genetics Laboratory, Advanced Biosciences Labs, Basic Research Program, National Cancer Institute, Frederick Cancer Research and Development Center, Frederick, Maryland 21702

Recent genetic analyses have revealed an important association of the gene encoding the P/Q-type voltage-dependent Ca^{2+} channel α_{1A} subunit with hereditary neurological disorders. We have identified the ataxic mouse mutation, *rolling Nagoya* (tg^{rol}), in the α_{1A} gene that leads to a charge-neutralizing arginine-to-glycine substitution at position 1262 in the voltage sensor-forming segment S4 in repeat III. Ca^{2+} channel currents in acutely dissociated Purkinje cells, where P-type is the dominant type, showed a marked decrease in slope and a depolarizing shift by 8 mV of the conductance–voltage curve and reduction in current density in tg^{rol} mouse cerebella, compared with those in wild-type. Compatible functional change was induced by the tg^{rol} mutation in the recombinant α_{1A} channel, indicating that a defect in voltage sensor of P/Q-type Ca^{2+} channels is the direct consequence of the tg^{rol} mutation. Furthermore, somatic whole-cell recording of mutant Purkinje cells displayed only abortive Na^+ burst activity and hardly exhibited Ca^{2+} spike activity in cerebellar slices. Thus, in tg^{rol} mice, reduced voltage sensitivity, which may derive from a gating charge defect, and diminished activity of the P-type α_{1A} Ca^{2+} channel significantly impair integrative properties of Purkinje neurons, presumably resulting in locomotor deficits.

Key words: P/Q-type Ca^{2+} channel; voltage sensor; gating charge; cerebellar Purkinje cells; ataxia; Ca^{2+} channel α_{1A} subunit

To evoke diverse cellular responses, Ca^{2+} influx across the plasma membrane makes a major contribution to augmenting the cytosolic free Ca^{2+} concentration (Clapham, 1995). Multiple voltage-gated Ca^{2+} channel types, including five high-threshold types (L, N, P, Q, and R) and the low-threshold T-type, form major Ca^{2+} entry pathways in neurons (Bean, 1989; Tsien et al., 1991; Llinás et al., 1992; Kobayashi and Mori, 1998). Several types of these Ca^{2+} channels are colocalized in a single neuron and are believed to contribute to fine tuning of neuronal activity, because each type is differently modulated. Although the critical role of Ca^{2+} channels, particularly the P- and N- types, for transmitter release in the synaptic terminals has been well established (Hirning et al., 1988; Turner et al., 1992; Takahashi and Momiyama, 1993; Artalejo et al., 1994; Regehr and Mintz, 1994), the roles of Ca^{2+} channels in integration of signals or synaptic plasticity have been poorly understood.

Voltage-gated Ca^{2+} channels are composed of the main pore-forming α_1 subunit, encoded by a family of genes (α_{1A}, α_{1B}, α_{1C}, α_{1D}, α_{1E}, α_{1F}, α_{1G}, α_{1H}, α_{1I}, and α_{1S}) (Kobayashi and Mori, 1998; Lee et al., 1999), and the accessory α_2/δ, β, and γ subunits (Campbell et al., 1988; Ahlijanian et al., 1990; Glossmann and Striessnig, 1990; Witcher et al., 1993; Letts et al., 1998). The α_{1A} subunit was originally characterized as a high-voltage-activated Ca^{2+} channel that is resistant to blockade by the N-type-selective inhibitor ω-conotoxin GVIA or the L-type inhibitor dihydropyridines (Mori et al., 1991). It is now accepted that P- and Q-types, which differ in sensitivity to ω-agatoxin-IVA (ω-Aga-IVA) and inactivation kinetics (Llinás et al., 1989; Regan et al., 1991; Mintz et al., 1992; Zhang et al., 1993), are produced from the single α_{1A} gene by alternative splicing (Mori et al., 1991; Sather et al., 1993; Bourinet et al., 1999) and/or through association with different isoforms of accessory subunits (Stea et al., 1994), although the mechanism by which different phenotypes are produced has not been fully explained yet (Bourinet et al., 1999).

Molecular genetic analyses have identified that mutations of the gene encoding the Ca^{2+} channel α_{1A} subunit cause cerebellar ataxia and other forms of neurological disorders. In the human α_{1A} gene, missense mutations, nonsense mutations, and CAG expansion have been shown to underlie neurological disorders such as familial hemiplegic migraine, episodic ataxia type-2 (Ophoff et al., 1996), and autosomal dominant spinocerebellar ataxia (SCA6) (Zhuchenko et al., 1997). Our characterization of the P/Q-type Ca^{2+} channels with an expanded stretch of 24, 30, or 40 polyglutamines revealed direct effects of polyglutamine expansion on channel properties (Matsuyama et al., 1999). To elucidate etiology of these human genetic channelopathies and to develop methods for treatments, the spontaneous mouse mutants of the α_{1A} subunit gene are useful models. A missense mutation was found in *tottering* (*tg*) mice, which display a delayed-onset, recessive disorder consisting of ataxia, paroxysmal dyskinesia, and absence seizure resembling petit mal epilepsy (Fletcher et al., 1996). The *tg* mutation causes substitution of leucine for proline at a position close to the conserved pore-lining region ("P" region) in the extracellular segment of the second of the four internal repeats (Fletcher et al., 1996). Mice with an allelic tottering mutation *leaner* (tg^{la}), which causes more severe symptoms, have a single nucleotide substitution

Received March 3, 2000; revised May 2, 2000; accepted May 15, 2000.

This work was supported by research grants from the Ministry of Education, Science, Sports, and Culture of Japan, by the Research Grant for Cardiovascular Diseases from the Ministry of Health and Welfare, by "the Research for the Future" program of the Japan Society for the Promotion of Science, and by the National Cancer Institute, Department of Health and Human Services, under contract with ABL. We thank Brian Seed and Gary Yellen for the CD8 expression plasmid, Kazuto Yamazaki for helpful advice, and Noboru Ogiso and Takeshi Hiroe for their assistance in providing mutant mice.

Correspondence should be addressed to Yasuo Mori, Department of Information Physiology, National Institute for Physiological Sciences, Okazaki, Aichi 444–8585, Japan. E-mail: moriy@nips.ac.jp.

 0270-6474/00/205654-09$15.00/0

at an exon/intron junction, which results in skipping the exon, or in failure to splice out the succeeding intron (Fletcher et al., 1996). In both cases, the tg^{la} mutation causes truncation of the normal open reading frame and expression of aberrant C-terminal sequences. Recent reports (Dove et al., 1998; Lorenzon et al., 1998; Wakamori et al., 1998) have demonstrated the causative relationship among the tottering mutations, the affected Ca^{2+} channel properties, and the neurological disorders, through comprehensive comparison of the mutant Ca^{2+} channel properties in native Purkinje cells of *tg* and tg^{la} mice in which many other factors can affect the channel phenotype, with those in the recombinant expression system, in which direct effects of the mutations can be evaluated precisely. Studies using the mutant mice provide important clues in understanding the roles of Ca^{2+} channels in integration of neuronal signaling.

Mouse mutation *rolling Nagoya* (tg^{rol}) has been reported as an allelic mutation of *tg* and tg^{la} (Oda, 1981). Homozygous tg^{rol} mutant mice show poor motor coordination of hindlimbs, and sometimes stiffness of the hindlimbs and tail, but no seizures (Oda, 1973, 1981). Here, we have identified a causative mutation in the α_{1A} subunit gene of the ataxic mouse tg^{rol} (Oda, 1973). Reduced voltage sensitivity and diminished activity of P/Q-type Ca^{2+} channels are the direct functional consequence of the tg^{rol} mutation. Our results also provide evidence that impairment of action potential generation in cerebellar Purkinje cells is a critical cerebellar defect that underlies the ataxic phenotype of tg^{rol} mice.

MATERIALS AND METHODS

Mice. The mutant gene, tg^{rol} (*rolling mouse Nagoya*) (Oda, 1973), was introduced into a C3H background by the cross–intercross matings, and a C3H-tg^{rol} congenic was established (Oda, 1981). The mice were provided with a commercial diet (CE-2; Nihon Clea, Tokyo, Japan) and water *ad libitum* under conventional conditions with controlled temperature, humidity, and lighting (22 ± 2°C, 55 ± 5%, and 12 hr light/dark cycle with lights on at 7:00 A.M.). The strains were maintained and propagated at the Laboratory of Animal Management, School of Agricultural Sciences, Nagoya University of Japan and at the National Institute for Physiological Sciences of Japan.

cDNA cloning and sequence analysis. cDNAs encoding the α_{1A} subunit were isolated through RT-PCR using cDNA amplification kit (Clontech, Palo Alto, CA), LA *Taq* (Takara, Otsu, Japan) and poly(A)$^+$ RNA from the brains of at least five mice for each of wild-type and mutant. PCR primers were designed according to the sequence by Fletcher et al. (1996) so that five 1200–1500 bp PCR fragments cover the whole 6495 bp reported sequence. Genomic DNA fragments containing the mutation site were isolated by PCR using La *Taq* (Takara) and genomic DNA from wild-type and tg^{rol} mice. cDNA and genomic clones were sequenced using an automated sequencer (model 373S; Perkin-Elmer, Norwalk, CT).

Northern blot analysis. RNA blot hybridization analysis was performed using 20 μg of total RNA from wild-type and tg^{rol} mouse brain. The probe was the DNA fragment carrying the nucleotide sequence 3439–4239 of the mouse α_{1A} subunit cDNA. Random primer DNA labeling kit version 2 (Takara) was used to prepare the ^{32}P-labeled probe. Hybridization was performed at 42°C in 50% formamide, 5× SSC, 50 mM sodium phosphate buffer, pH 7.0, 0.1% SDS, 0.1% polyvinylpyrrolidone, 0.1% Ficoll 400 (Pharmacia Biotech, Uppsala, Sweden), 0.1% bovine serum albumin, and 0.2 mg/ml sonicated herring sperm DNA, as described previously (Mori et al., 1991).

Construction of expression plasmids encoding Ca^{2+} channel α_{1A} subunit with tg^{rol} mutation. For construction of expression cDNA encoding the tg^{rol}-α_{1A} (BI-2) subunit mutant, a PCR fragment amplified using pSPCBI-2 (Mori et al., 1991) as a template, a primer BIPMI(+) (5′-ACCACACC GTGGTCCAAGTGAACAAAAATG-3′) (sense) and a primer 2Nag(−) (5′-GAGCTTTGGCAACCCCTTGATGGTTTTGAG -3′) (antisense), and a PCR fragment amplified using pSPCBI-2, and a primer 2Nag(+) (5′-CAAAACCATCAAGGGGTTGCCAAAGCTC -3′)(sense) and a primer BIAclI(-) (5′-GAAGTAGACCACGTAGAAGATGGACATCTC-5′) (antisense), were combined with the primers BIPMI(+) and BIAclI(-) in the subsequent PCR. The PCR product was digested with *Pfl*MI and *Acc*I, and the yielded fragment with the mutation was substituted for the corresponding *Pfl*MI(3574)/*Acc*I(4506) sequence of the rabbit α_{1A} (BI-2) cDNA in the recombinant plasmid pK4KBI-2 (Niidome et al., 1994) to obtain pK4KBI-tg^{rol}.

Expression of recombinant α_{1A} Ca^{2+} channels in baby hamster kidney cells. To have a direct comparison of functional effects caused by different α_{1A} mutations, the tg^{rol} mutant was expressed in the same environment, namely, in the presence of the same accessory subunits, as those used for expression of the *tg* and tg^{la} mutants (Wakamori et al., 1998). Baby hamster kidney (BHK) cells were transfected with the pAGS-3 recombinant plasmid pAGS-3a2 (Klöckner et al., 1995) and pCABE (Niidome et al., 1994) using the $CaPO_4$ protocol (Chen and Okayama, 1987), and were cultured in DMEM containing G-418 (600 μg/ml) (Life Technologies, Gaithersburg, MD), to first establish a BHK line, BHK6, with stable expression of the α_2/δ and β_{1a} subunits. To transiently express normal or tg^{rol} mutant α_{1A} channels, BHK6 cells were transfected with the recombinant plasmid pK4KBI or pK4KBI-tg^{rol} plus πH3-CD8 containing the cDNA of the T-cell antigen CD8 (Jurman et al., 1994). Transfection was performed using SuperFect Transfection Reagent (Qiagen, Hilden, Germany). Cells were trypsinized, diluted with DMEM containing 10% fetal bovine serum (FBS), 30 U/ml penicillin, and 30 μg/ml streptomycin, and plated onto Celldesk (Sumitomo Bakelite, Tokyo, Japan) 18 hr after transfection. Then cells were subjected to measurements 48–66 hr after plating on the coverslips. Cells expressing α_{1A} channels were selected through detection of CD8 coexpression using polystyrene microspheres precoated with antibody to CD8 (Dynabeads M-450 CD8; Dynal, Oslo, Norway).

Preparation of dissociated Purkinje cells. Purkinje cells were freshly dissociated from 18- to 30-d-old mice. The procedure for obtaining dissociated cells from mice is similar to that described elsewhere (Wakamori et al., 1993). Coronal slices (400-μm-thick) of cerebellum were prepared using a microslicer (DTK-1000, Dosaka, Kyoto, Japan). After preincubation in Krebs' solution for 40 min at 31°C, the slices were digested: first in Krebs' solution containing 0.01% pronase (Calbiochem–Novabiochem, La Jolla, CA) for 25 min at 31°C and then in solution containing 0.01% thermolysin (type X; Sigma, St. Louis, MO) for 25 min at 31°C. The Krebs' solution used for preincubation and digestion contained the following (in mM): 124 NaCl, 5 KCl, 1.2 KH_2PO_4, 2.4 $CaCl_2$, 1.3 $MgSO_4$, 26 $NaHCO_3$, and 10 glucose. The solution was continuously oxygenated with 95% O_2 and 5% CO_2. Then the brain slices were punched out and dissociated mechanically by the use of fine glass pipettes having a tip diameter of 100–200 μm. Dissociated cells settled on tissue culture dishes (Primaria #3801; Nippon Becton Dickinson, Tokyo, Japan) within 30 min. Purkinje cells were identified by their large diameter and characteristic pear shape because of the stump of the apical dendrite. To make a sufficient space-clamp of the Purkinje cell body, Purkinje cells lacking most of dendrites were used throughout the present experiments.

Whole-cell recordings. Electrophysiological measurements were performed on Purkinje cells and BHK cells. Currents were recorded at room temperature (22–25°C) using whole-cell mode of the patch-clamp technique (Hamill et al., 1981) with an Axopatch 200B patch-clamp amplifier (Axon Instruments, Foster City, CA). Patch pipettes were made from borosilicate glass capillaries (1.5 mm outer diameter and 0.87 mm inner diameter; Hilgenberg, Malsfeld, Germany) using a model P-87 Flaming–Brown micropipette puller (Sutter Instrument, San Rafael, CA). The patch electrodes were fire-polished. Pipette resistance ranged from 1 to 2 MΩ when filled with the pipette solutions described below. The series resistance was electronically compensated to >70%, and both the leakage and the remaining capacitance were subtracted by -P/6 method. Currents were sampled at 100 kHz after low-pass filtering at 10 kHz (−3 dB) using the 8-pole Bessel filter (model 900; Frequency Devices, Haverhill, MA) in the experiments of activation kinetics, otherwise sampled at 10 kHz after low-pass filtering at 2 kHz (−3 dB). Data were collected and analyzed using the pClamp 6.02 software (Axon Instruments). Ba^{2+} currents were recorded in an external solution that contained (in mM): 3 $BaCl_2$, 155 tetraethylammonium chloride (TEA-Cl), 10 HEPES, and 10 glucose, pH adjusted to 7.4 with TEA-OH. The pipette solution contained (in mM): 85 Cs-aspartate, 40 CsCl, 2 $MgCl_2$, 5 EGTA, 2 ATPMg, 5 HEPES, and 10 creatine-phosphate, pH adjusted to 7.4 with CsOH. The junction potential between the Cs-based internal solution and the external recording solution was 10 mV. Correction for this potential would have shifted all voltage dependence by 10 mV forward more negative potentials. In the experiments with ω-Aga-IVA, the external solution was always supplemented with 0.1 mg/ml cytochrome c. Cytochrome c at 0.1 mg/ml had no effect on Ba^{2+} currents. Rapid application of drugs were made by a modified "Y-tube" method. Details of this technique have already appeared (Wakamori et al., 1998). The external solution surrounding a cell recorded was completely exchanged within 200 msec.

All values are given as mean ± SE. Statistical comparison between normal and mutant mice or mutant channels was performed by Student's *t* test ($^*p < 0.05$; $^{**}p < 0.01$).

Slice preparation. Firing pattern of the cerebellar Purkinje cells were measured using 400-μm-thick parasagittal cerebellar slices from 2- to 3-week-old normal and homozygous tg^{rol} mice. Slices were cut in ice-cold solution using the microslicer. They were incubated at 32°C for 1 hr for recovery and thereafter maintained at room temperature. The solution used for slicing and for perfusion during measurement contained (in mM): 125 NaCl, 25 $NaHCO_3$, 25 glucose, 2.5 KCl, 1.25 NaH_2PO_4, 2 $CaCl_2$, and 1 $MgCl_2$, pH 7.4 when bubbled with 95% O_2 and 5% CO_2. Slices were mounted on an upright microscope (Axioskop FS; Zeiss, Oberkochen, Germany). Neurons were visually identified using infrared differential interference contrast video microscopy (C2400–07; Hamamatsu Photonics, Hamamatsu, Japan).

Somatic whole-cell voltage recording. Somatic whole-cell voltage recordings in the current-clamp mode were made with 4–8 MΩ patch pipettes using an EPC-7 amplifier (List, Darmstadt, Germany). The patch-clamp amplifier was controlled by a computer using the Pulse software package (Heka, Lambrecht, Germany). The pipette solution contained (in mM): 115 potassium gluconate, 20 KCl, 4 Mg-ATP, 10 phosphocreatine, 0.3 GTP, and 10 HEPES, pH 7.2 adjusted with KOH. Purkinje neurons typically had

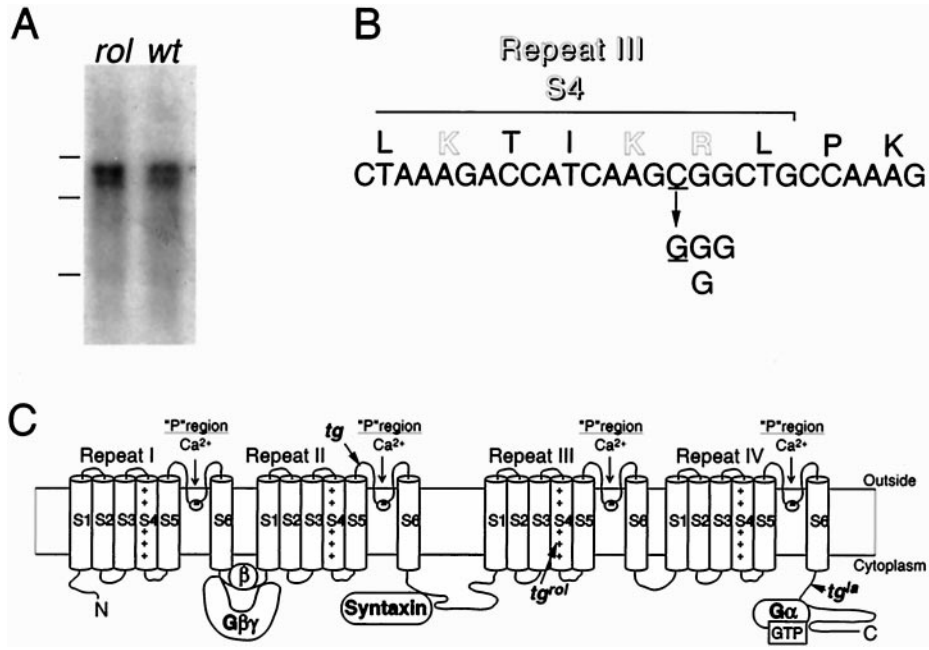

Figure 1. Determination of tg^{rol} mutation. *A*, Expression of the Ca^{2+} channel α_{1A} subunit mRNA in the tg^{rol} (*rol*) and wild-type (wt) mouse brain. Molecular weight markers are RNAs of 9.5, 7.5, and 4.4 kb. *B*, The sequence alteration in the tg^{rol} mutant. tg^{rol} contains a cytosine (*C*) to thymidine (*T*) change at nucleotide position 3784, which results in an arginine (*R*) to glycine (*G*) alteration at amino acid position 1262. *C*, Proposed transmembrane topography of the α_{1A} subunit and positions of tg^{rol} and the other two α_{1A} mutations (indicated by *arrows*).

resting membrane potential levels between −60 and −70 mV. Action potentials were evoked by short and small depolarizing current injections (200 msec; 100–300 pA), or long and large depolarizing current injections (1.2 or 20 sec; 800–1500 pA) from somatic patch pipettes. Experiments were done at 32°C. To evoke Ca^{2+} spikes, it was necessary to raise the temperature to 32°C.

Histochemistry. Animals were anesthetized with sodium pentobarbitone and perfused transcardially with 4% paraformaldehyde in 0.1 M sodium phosphate buffer. Dissected tissue was post-fixed overnight at 4°C, embedded in paraffin, and sliced at 5 μm for cresyl violet or hematoxylin eosin staining. For immunocytochemistry, brains were cryoprotected in 30% sucrose, frozen, and cut at 75 μm on a Leitz sliding microtome. Primary antibody to tyrosine hydroxylase (TH) was used at dilution of 1:500, and the secondary antibody was previously described (Fletcher et al., 1996).

RESULTS

Determination of the structural defect in the tg^{rol} mouse α_{1A} subunit

The previous mating test between the heterozygous *rolling Nagoya* ($+/tg^{rol}$) and the heterozygous *tottering* ($+/tg$) mice has given frequency of ataxic offspring that satisfactorily agree with the assumption that tg^{rol} and *tg* mutations are allelic (Oda, 1981). Northern blot analysis of brain RNA failed to detect any differences in transcript structure of the α_{1A} subunit between wild-type and tg^{rol} mice: ~8.2 and ~9.2 kb bands were observed at similar intensity in the wild-type and mutant (Fig. 1*A*). The tg^{rol} mutation was therefore identified through cloning of mouse α_{1A} subunit cDNA from the tg^{rol} mouse brain by RT-PCR. Sequence analysis revealed a C-to-G change at nucleotide residue 3784 (Fig. 1*B*). This was the only nucleotide alteration found consistently throughout the α_{1A} subunit cDNA obtained from the homozygous (tg^{rol}/tg^{rol}) mice, that unequivocally showed ataxic phenotype, and either C or G was found at the position 3784 in the α_{1A} sequence from heterozygous ($tg^{rol}/+$) mice. Both types of splice variation, $\alpha_{1A\text{-}a}$ or $\alpha_{1A\text{-}b}$, were found at the three different sites (Bourinet et al., 1999) in the isolated cDNA fragments, revealing no specific link between particular splice variants and C3784G substitution. The nucleotide substitution C3784G was identified also in the genomic α_{1A} sequence. The mutation leads to a nonconservative, charge-neutralizing arginine (R)-to-glycine (G) substitution at the amino acid position 1262. R1262 is near the C-terminus of repeat III S4 (Fig. 1*B,C*), being deviated from the characteristic arrangement of the positively charged amino acids located at every third position in the voltage-sensing region S4.

Direct functional impact of the tg^{rol} mutation on the recombinant α_{1A} channels

The molecular nature of the amino acid substitution induced by the tg^{rol} mutation suggests that voltage-sensing function is altered in the P/Q-type Ca^{2+} channel. We therefore examined the direct functional impact of the tg^{rol} R1262G substitution by introducing the C-to-G mutation at the corresponding site of the rabbit α_{1A} subunit BI-2 (Mori et al., 1991). The control wild-type and tg^{rol} mutant α_{1A} cDNAs were inserted in the pK4K plasmid (Niidome et al., 1994) and were transiently expressed in the BHK6 cells, which stably express the Ca^{2+} channel α_2/δ and β_{1b} subunits (Wakamori et al., 1998). When membrane potential was stepped from a holding potential (V_h) of −100 mV to a test pulse of 0 or 10 mV using whole-cell patch clamp method, the average peak current density for the tg^{rol}-α_{1A} channel was significantly smaller (14.7 ± 3.5 pA/pF; $n = 30$) ($p < 0.001$) than that for the wild-type α_{1A} channel (52.7 ± 6.6 pA/pF; $n = 37$) in the solution containing 3 mM Ba^{2+} (Fig. 2*A*). Current-voltage (*I–V*) relationships for the wild-type and mutant α_{1A} Ba^{2+} currents indicated that the wild-type and mutant α_{1A} channels were activated by step depolarization above −30 mV from a V_h of −100 mV (Fig. 2*B,C*). The current amplitude increased with increments of depolarization, reaching peaks in the *I–V* relationships around 0 and 10 mV for the wild-type α_{1A} channel and the tg^{rol}-α_{1A} channel, respectively (Fig. 2*D*). The activation curves, obtained by fitting peak of tail currents at the fixed potential of −50 mV after 5 msec step depolarization from −50 to 30 mV with 5 mV increments with a single Boltzmann function, showed different voltage dependence between the wild-type and mutant α_{1A} channels (Fig. 2*E*): the voltage dependence of activation was shifted in the depolarizing direction and showed reduction of slope in the mutant channel. The midpoint of the activation curve was −10.2 ± 0.7 mV for the wild-type α_{1A} channel ($n = 12$) and 0.8 ± 1.0 mV for the tg^{rol}-α_{1A} channel ($n = 17$; $p < 0.001$), and the slope factor changed from 5.4 ± 0.3 mV in the wild-type α_{1A} channel to 7.4 ± 0.2 mV in the tg^{rol}-α_{1A} channel ($p < 0.001$). The change of the slope factor was confirmed by the limiting slope analysis, where the limiting slope of semilogarithmic tail activation curves for the tg^{rol} α_{1A} channel was clearly shallower than that for the wild-type α_{1A} channel (Fig. 2*E*). The voltage dependence of inactivation was determined by the use of 2 sec prepulses to a series of different potentials followed by the test pulse to 0 or 10 mV for the normal and tg^{rol} α_{1A} channels, respectively. Peak

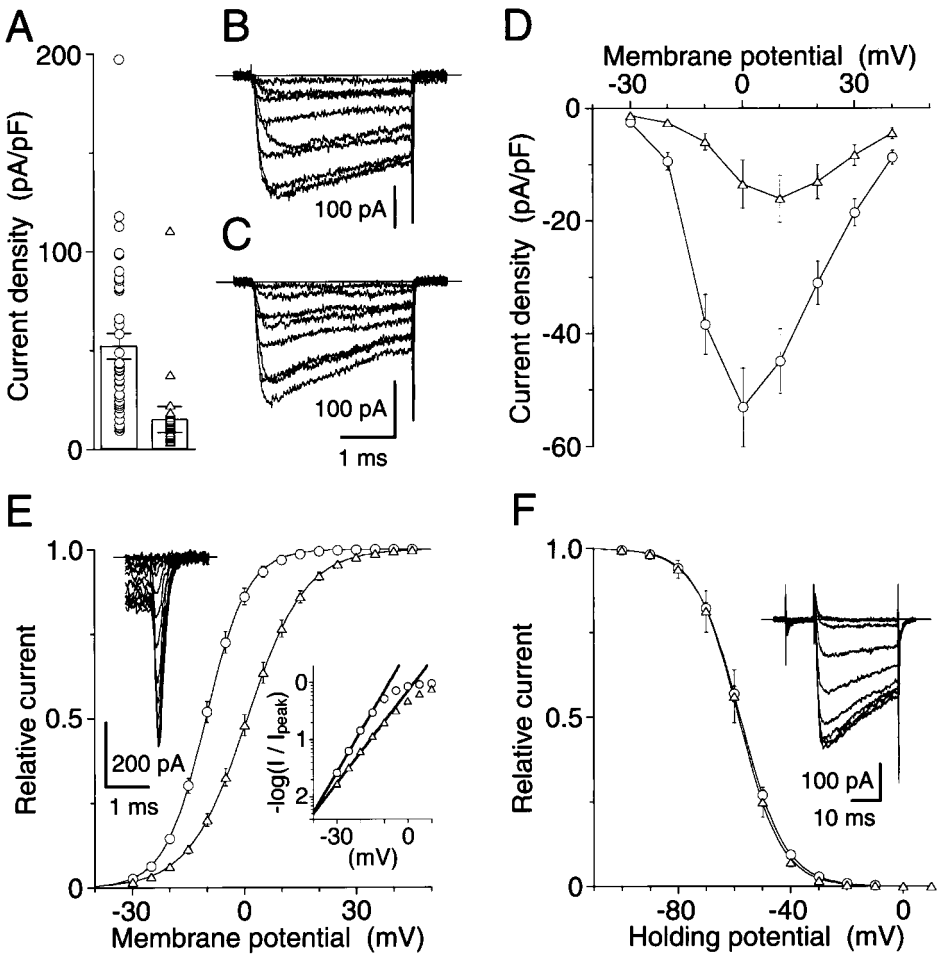

Figure 2. Comparison of Ba^{2+} currents in BHK cells recombinantly expressing the wild-type and mutant α_{1A} channels. *A*, Distribution of peak current density. Individual values of Ba^{2+} currents in BHK cells expressing wild-type (*open circle*) and tg^{rol} α_{1A} channels (*open triangle*) and their means (*open box*) ± SE are shown. *B–D*, Current–voltage relationships. Families of Ba^{2+} currents evoked by 30 msec depolarizing pulses from −30 to 40 mV for the wild-type channel (*B*) and the tg^{rol} α_{1A} channel (*C*) with 10 mV increments from a V_h of −100 mV. Current density was plotted against membrane potential (*D*). Each point represents an average value from 34 experiments of the wild-type α_{1A} channel and 25 experiments of the tg^{rol} α_{1A} channel. *E*, Activation curves. *Left inset*, Superimposed tail currents elicited by repolarization to −50 mV after the 5 msec test pulse from −30 to 40 mV with increments of 5 mV in a BHK expressing the tg^{rol} α_{1A} channel. Amplitudes of tail currents were normalized to the tail current amplitude obtained with a test pulse to 40 mV. The mean values from 12 experiments of the wild-type α_{1A} channel and 17 experiments of the tg^{rol} α_{1A} channel were plotted against test pulse potentials and fitted to the Boltzmann equation with a midpoint ($V_{0.5}$) of −10.3 mV and a slope factor (k) of 5.6 mV for the wild-type α_{1A} channel and a $V_{0.5}$ of 0.7 mV and a k of 7.8 mV for the tg^{rol} α_{1A} channel. *Right inset*, The activation curves plotted semilogarithmically, with lines corresponding to slopes of 6.1 and 8.1 mV per *e*-fold change for the wild-type and tg^{rol} α_{1A} channels, respectively. *F*, Inactivation curves. *Inset* shows Ba^{2+} currents evoked by 20 msec test pulse to 10 mV after the 10 msec repolarization to −100 mV after 2 sec V_h displacement from −100 to −20 mV with 10 mV increments in a BHK expressing the tg^{rol} α_{1A} channel. Amplitudes of currents evoked by the test pulses were normalized to the current amplitude induced by the test pulse after a V_h replacement of −100 mV. The mean values from 12 BHK cells expressing the wild-type α_{1A} channel and 7 BHK cells expressing the tg^{rol}-α_{1A} channel were plotted as a function of potentials of the 2 sec V_h displacement, and were fitted to the Boltzmann equation. $V_{0.5}$ and k were −58.4 and 7.6 mV for the wild-type α_{1A} channel and −57.9 and 7.9 mV for the tg^{rol} α_{1A} channel, respectively. Error bars indicate mean ± SE if they are larger than symbols.

current amplitudes were normalized to the peak current amplitude induced by the test pulse from a prepulse potential of −100 mV and were plotted against the prepulse potentials. The estimated half-inactivation potential and the slope factor of the inactivation curves fitted by a Boltzmann equation were −57.9 ± 0.2 mV and 7.8 ± 0.3 mV in the wild-type α_{1A} channel (n = 12), and −58.7 ± 2.4 mV and 6.8 ± 0.3 mV in the tg^{rol}-α_{1A} channel (n = 7), respectively (Fig. 2*F*), revealing that voltage dependence of inactivation was unaffected by the tg^{rol} mutation. Thus, our results strongly suggest that the tg^{rol} mutation, which cause charge-neutralizing amino acid substitution in repeat III S4, leads to alteration in voltage-sensing function of the P/Q-type α_{1A} Ca^{2+} channels in the recombinant system.

Electrophysiological characterization of native P-type Ca^{2+} channel currents in Purkinje cells from tg^{rol} mice

We next electrophysiologically characterized P/Q-type Ca^{2+} channels in native preparation from wild-type and homozygous tg^{rol} mice, so that functional alteration induced by R1262G substitution in the recombinant α_{1A} channels can be compared with functional defects of native tg^{rol} P/Q-type channels. The P-type channel is elicited by the splice variant of α_{1A} subunit in cerebellar Purkinje cells (Mori et al., 1991; Fujita et al., 1993; Bourinet et al., 1999). Ba^{2+} currents, evoked by step pulses at −20 or −10 mV from a V_h of −80 mV in cerebellar Purkinje cells freshly dissociated from 18 to 40 d homozygous *rolling* (tg^{rol}) mice (n = 7) and normal wild-type (n = 15), were first examined for the sensitivity to the P/Q-type Ca^{2+} channel-selective inhibitor, ω-Aga-IVA (Mintz et al., 1992). Concentrations of 10 and 30 nM ω-Aga-IVA reduced Ba^{2+} currents to 17.1 ± 1.8% (n = 9) and 6.8 ± 2.6% (n = 6) for normal and 25.6 ± 4.3% (n = 5) and 4.6 ± 0.5% (n = 4) for tg^{rol} Purkinje cells, respectively. After a tetanic stimulation (30 times to 150 mV for 10 msec at 10 Hz), current amplitude recovered to 84.8 ± 6.1% of control in tg^{rol} mice. Thus, P-type is the major high threshold channel in tg^{rol} cerebellar Purkinje cells as in wild-type Purkinje cells (Mintz et al., 1992).

The mean amplitude of Ba^{2+} currents, elicited by a step pulse from a V_h of −80 to −10 mV, was significantly smaller for tg^{rol} mice (3.41 ± 0.18 nA; n = 32) than that elicited by a step pulse to −20 mV for normal mice (4.93 ± 0.27 nA; n = 73) in the solution containing 3 mM Ba^{2+} (Fig. 3*A*) ($p < 0.001$). The cell capacitance, which can be an index of the cell size, for tg^{rol} mice (13.1 ± 0.6 pF) was statistically ($p < 0.01$) smaller than that for normal mice (15.4 ± 0.5 pF) (Fig. 3*B*). Reduction in current amplitude is not only attributable to smaller sizes of Purkinje neuron cell bodies, as the current density obtained by dividing current amplitude by cell capacitance was also significantly ($p < 0.001$) smaller for tg^{rol} mice (247 ± 14 pA/pF) than that for normal wild-type mice (325 ± 17 pA/pF) (Fig. 3*C*). These results suggest that the tg^{rol} mutation disrupts function and cellular development, as well, of Purkinje cells.

Ca^{2+} channel currents elicited by test pulses from a V_h of −80 mV in Purkinje cells from normal and mutant mice are shown in Figure 3, *D* and *E*, respectively. The threshold potentials to evoke inward currents were around −40 mV for both normal and tg^{rol} mice, whereas the potentials giving peak amplitudes were −20 mV for normal mice and −10 mV for tg^{rol} mice (Fig. 3*F*). The voltage dependence of activation was evaluated by measuring tail currents as in recombinant channels (Fig. 3*G*). The activation curve, which

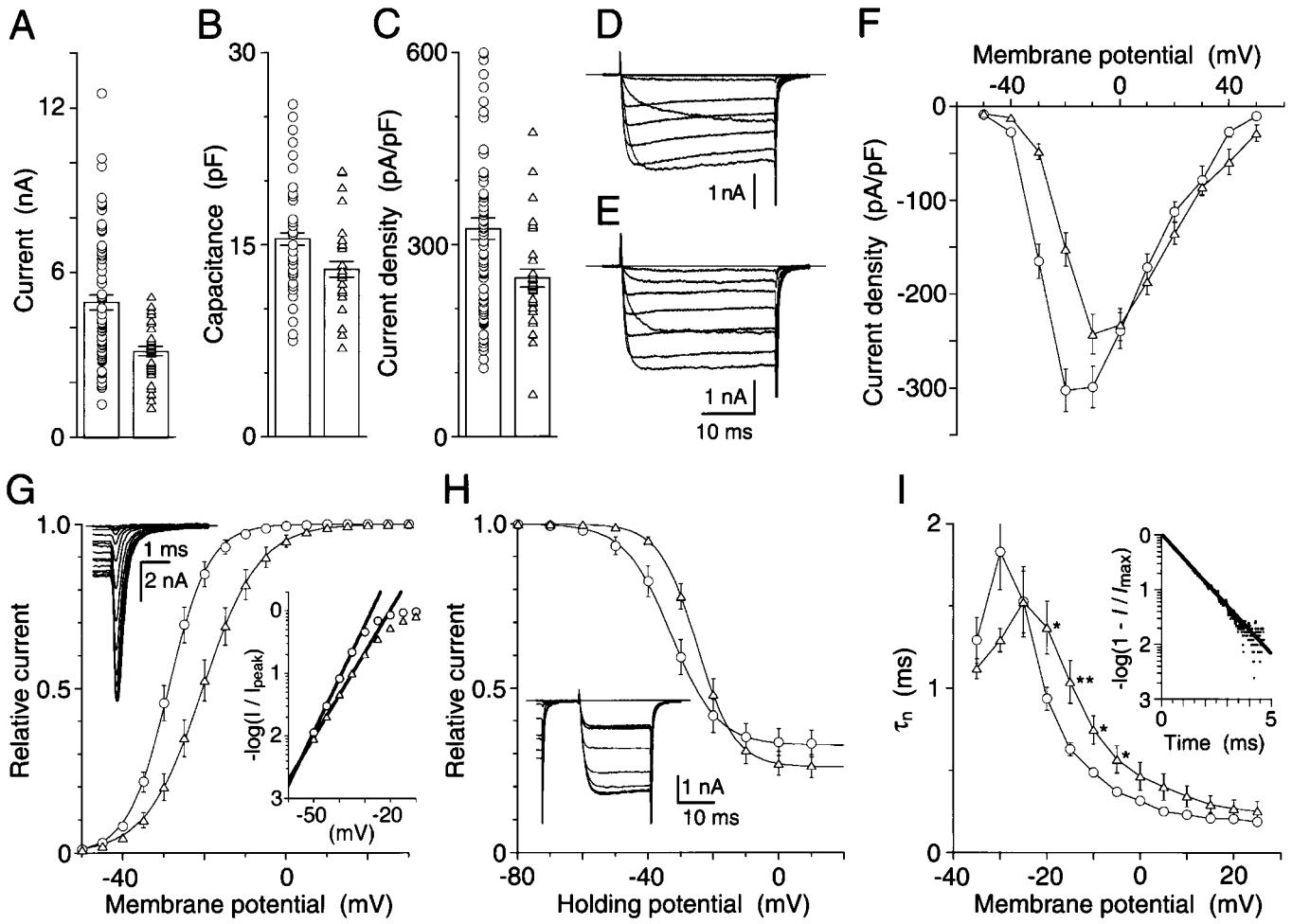

Figure 3. Comparison of Ca^{2+} channel currents recorded in Purkinje cells dissociated from normal and tg^{rol} mice. Distribution of peak current amplitude (*A*), cell capacitance (*B*), and current density (*C*). Individual values of Ca^{2+} channel currents in wild-type (open circle) and mutant Purkinje cells (*open triangle*) and their means (*open box*) ± SE are shown. Families of Ba^{2+} currents evoked by 30 msec depolarizing pulses from −50 to 20 mV for normal mice (*D*) and from −40 to 30 mV for tg^{rol} mice (*E*) with 10 mV increments from a holding potential (V_h) of −80 mV. Current density was plotted against membrane potential (*F*). Each point represents an average value of 39 and 24 Purkinje cells from normal and tg^{rol} mice, respectively. *G*, Activation curves. Left inset, Superimposed tail currents elicited by repolarization to −60 mV after the 5 msec test pulse from −50 to 20 mV with increments of 5 mV in a tg^{rol} Purkinje cell. Amplitudes of tail currents were normalized to the tail current amplitude obtained with a test pulse to 30 mV. The mean values from 8 normal and 13 tg^{rol} Purkinje cells were plotted against test pulse potentials and fitted to the Boltzmann equation with a $V_{0.5}$ of −28.9 mV and a k of 4.9 mV for normal mice and a $V_{0.5}$ of −20.5 mV and a *k* of 6.9 mV for tg^{rol} mice. *Right inset*, The semilogarithmic plots of activation curves, with lines corresponding to slopes of 5.1 and 6.4 mV per e-fold change for the wild-type and tg^{rol} Ca^{2+} channel currents, respectively. *H*, Inactivation curves. *Inset* shows Ba^{2+} currents evoked by 20 msec test pulse to −10 mV after the 10 msec repolarization to −80 mV after 2 sec V_h displacement from −80 to 10 mV with 10 mV increments in a tg^{rol} Purkinje cell. Amplitudes of currents evoked by the test pulses were normalized to the current amplitude induced by the test pulse after a V_h replacement of −80 mV. The mean values from 13 normal and 12 tg^{rol} Purkinje cells were plotted as a function of potentials of the 2 sec V_h displacement. The inactivating component (67% for normal mice and 74% for tg^{rol} mice) was fitted to the Boltzmann equation with a $V_{0.5}$ of −33.0 mV and a *k* of 7.1 mV for normal mice and a $V_{0.5}$ of −25.0 mV and a *k* of 5.8 mV for tg^{rol} mice. Error bars indicate mean ± SE if they are larger than symbols. *I*, Comparison of activation kinetics. Activation time constants were obtained from single-exponential fits of activation phase during 5 msec depolarizing steps. Data are expressed as mean ± SE of 8–14 Purkinje neurons. Error bars indicate mean ± SE if they are larger than symbols. Inset, Single-exponential fit (τ = 0.99 msec) of activation phase of Ba^{2+} currents evoked at −15 mV in a tg^{rol} Purkinje cell.

could be described by a single Boltzmann function, displayed a midpoint of −28.6 ± 0.9 mV and a slope factor of 4.6 ± 0.4 mV (n = 8) for normal mice, whereas that for tg^{rol} mice was shifted in the depolarizing direction (midpoint, −20.3 ± 1.7 mV; n = 13, $p <$ 0.001) and had a shallower voltage dependence (slope factor, 5.8 ± 0.2 mV; $p < 0.05$). The limiting slope analysis confirms the reduced steepness of slope of activation curve in tg^{rol} mice (Fig. 3*G*).

Voltage dependence of the inactivating component induced by the 2 sec displacements was fitted by the Boltzmann equation (Fig. 3*H*). The midpoint shifted from −33.4 ± 2.5 mV in normal mice (n = 13) to −24.8 ± 1.1 mV in tg^{rol} mice (n = 12; $p < 0.01$), but the slope factor was unaffected by the mutation (5.3 ± 0.6 mV for normal mice and 5.4 ± 0.4 mV for tg^{rol} mice). The fraction of inactivating component for tg^{rol} mice (74 ± 3%) was statistically similar to that for normal mice (67 ± 4%) ($p > 0.05$).

The time course of activation of inward currents was well described by a single exponential. The time constant plotted against different voltages was "bell-shaped" for normal mice and tg^{rol} mice. (Fig. 3*I*) For the wild-type and tg^{rol} currents, activation kinetics was the slowest at −30 and −25 mV, respectively, where almost half of the channels were activated. The voltage dependence of activation time constant for tg^{rol} currents was shifted in the depolarizing direction by 5 or 10 mV compared to that for the wild-type: at membrane potentials between −20 and −5 mV, activation speed of Ca^{2+} channels in tg^{rol} Purkinje cells was significantly slower than that in normal Purkinje cells. This is consistent with the depolarizing shift in the activation curve (Fig. 3*G*). Thus, the results demonstrate that voltage dependence of activation is similarly altered in the recombinant mutant α_{1A} channel and in native P-type channel in tg^{rol} Purkinje cells, suggesting that reduced voltage sensitivity of activation is the direct functional consequence of tg^{rol} mutation.

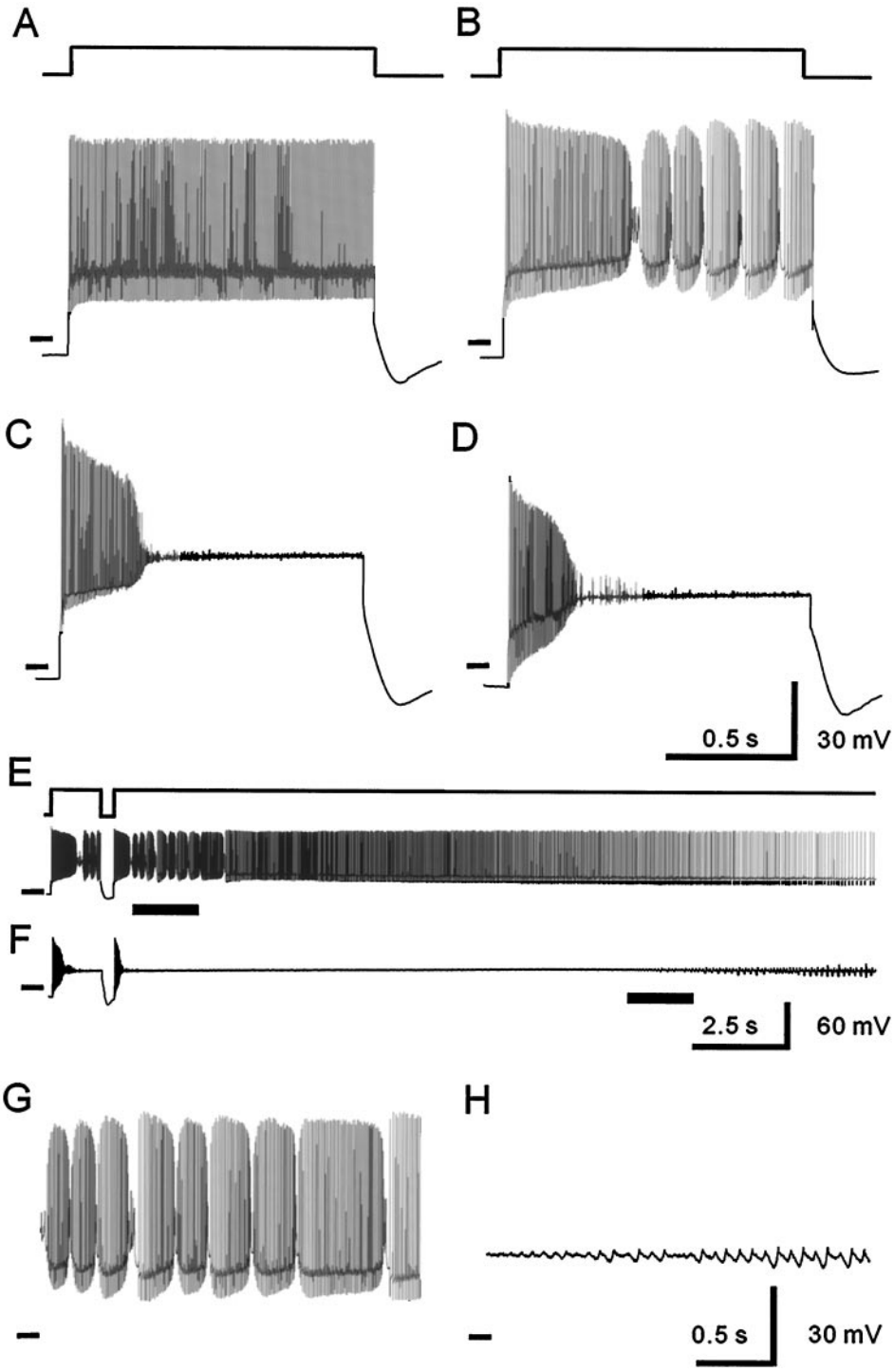

Figure 4. Firing patterns of Purkinje neurons of normal and *tg*^{rol} mice. *A*, Na^+ spikes in a normal Purkinje neuron evoked by injecting depolarizing current (1000 pA). B, Oscillatory response of Na^+ and Ca^{2+} spikes in normal Purkinje neuron evoked by injection of depolarizing current (1200 pA). *C*, Na^+ spikes were terminated in a normal Purkinje neuron during the depolarizing current injection (1000 pA) in the presence of 50 μM Cd^{2+} in the extracellular solution. *A–C* from different cells. *D*, Na^+ spikes were terminated in a Purkinje neuron from *tg*^{rol} mice even during the current injection (1000 pA). Calibration is common to *A–D*, Firing patterns of normal (*E*) and *tg*^{rol} (*F*) Purkinje neurons with very long injection of depolarizing currents (E, 1000 pA; *F*, 1200 pA). *G*, Oscillatory response of Na^+ and Ca^{2+} spikes observed in a normal Purkinje neuron. Expanded trace of *E* (marked with a *bar*). *H*, Ca^{2+} spikes observed in a *tg*^{rol} Purkinje neuron. Expanded trace of *F* (marked with a *bar*). A small bar at the beginning of each trace indicates the membrane potential of −60 mV. Depolarizing currents were injected from somatic patch pipettes.

Firing pattern of *tg*^{rol} cerebellar Purkinje neurons

To see the effect of the mutated Ca^{2+} channel property on the firing pattern of cerebellar Purkinje neurons, voltage recordings were performed using brain slice preparations. When small amounts of depolarizing current were injected to Purkinje cells through somatic patch pipettes, Purkinje neurons in normal and homozygous *tg*^{rol} mice showed similar firing patterns (data not shown). When larger amounts of depolarizing current were injected for a long period, wild-type Purkinje neurons exhibited bursts of Na^+ action potentials (Fig. 4*A*) (Llinás and Sugimori, 1980). During the Na^+ bursts, the membrane potential level between action potentials remained relatively polarized, preventing Na^+ channels from complete inactivation. Addition of Cd^{2+} caused depolarization of the interspike membrane potential and termination of bursting activity (Fig. 4*C*), suggesting that Ca^{2+}-activated K^+ channels are responsible for maintaining the polarized membrane potential during the bursts (Llinás and Sugimori, 1980). In 15 of the 21 cells examined, the Na^+ bursts lasted the whole 1.2 sec stimulation, but occasionally the Na^+ burst activity ceased and Ca^{2+} spikes appeared (6 of 21 cells) (Fig. 4*B*). Application of longer (10 sec) depolarizing current injections generated the Ca^{2+} spike activity in four of five cells (Fig. 4*E,G*). The Ca^{2+} spike activity, which often leads to oscillating behavior of Na^+ spike bursts and Ca^{2+} spikes, disappeared after application of Cd^{2+}. In contrast to wild-type, all the 13 Purkinje cells from homozygous *tg*^{rol} mice showed only abortive Na^+ burst activity during the 1.2 sec depolarizing current injections (Fig. 4*D*). On current injections, the interspike membrane potential level became

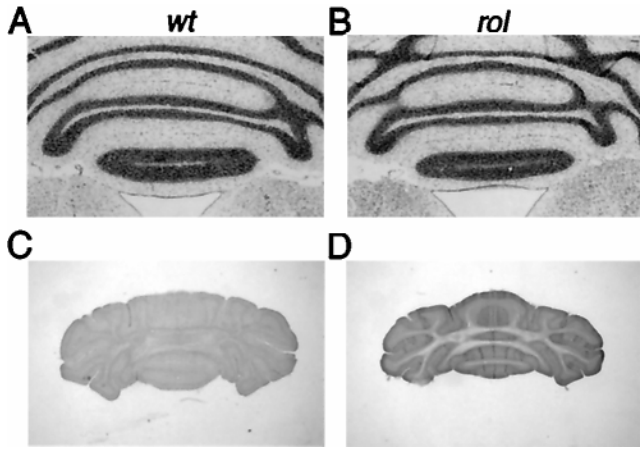

Figure 5. Histochemical characterization of tg^{rol} cerebellum. Nissl staining of wild-type (*wt*) (*A*) and tg^{rol} (*rol*) cerebella (*B*), and TH expression in wild-type (*C*) and tg^{rol} cerebella (*D*).

quickly depolarized, causing complete inactivation of Na^+ channel. This abortive Na^+ burst activity was similar to that observed in normal Purkinje cells in the presence of Cd^{2+} (Fig. 4*C*). The tg^{rol} Purkinje neurons hardly exhibited Ca^{2+} spike activity during 1.2 or 20 sec depolarization, but it was observed when even longer depolarization (~20 sec) was applied (Fig. 4*F,H*). The Ca^{2+} spike activity was oscillatory and occasionally accompanied by several Na^+ action potentials (two of six cells), but full bursts of Na^+ spikes were not evoked, presumably because of inactivation of Na^+ channels during long depolarization.

Histochemical characterization of tg^{rol} cerebellum

We further examined whether the tg^{rol} cerebella display characteristic pathophysiological properties that differ from those of the tg^{la} and *tg* mutants, in addition to the direct structural and functional impacts on P/Q-type Ca^{2+} channels. The brain sections from tg^{rol} mice were examined by staining with various immunohistochemical markers. Two conflicting papers were previously published on the granule cell loss in the tg^{rol} cerebellum (Nishimura, 1975; Mukaiyama and Mizuno, 1976). In the tg^{rol} cerebellar sections we examined (Fig. 5*B*), Nissl staining revealed normal cell density and no obvious decrease in size of granule cell layers, in contrast to the extensive granule cell loss in the tg^{la} sections (Fletcher et al., 1996). It has been reported that in the tg^{la} cerebellum, progressive apoptotic death of granule cells that may derive from misregulation of Ca^{2+} homeostasis by the tg^{la} mutant P/Q-type Ca^{2+} channels (Fletcher et al., 1996). However, the terminal deoxynucleotidyl transferase-mediated biotinylated dUTP nick end labeling assay detected no significant apoptotic cells in the tg^{rol} cerebellum, and the calbindin staining showed no apparent Purkinje cell loss (data not shown). In contrast to these differences among cerebella of the α_{1A} mutants, two populations of Purkinje cells were distinguished in tg^{rol} cerebella, as previously reported in the tg^{la} and *tg* cerebella (Hess and Wilson, 1991; Fletcher et al., 1996). Expression of TH, a key enzyme in the noradrenergic biosynthesis pathway whose expression is normally transient and is no longer detected in adult, showed a stripe pattern in mutant cerebella. The persistent expression of TH may be consistent with Ca^{2+} misregulation, considering the responsiveness of the TH promoter to Ca^{2+}, neuronal activity, and c-*fos* (Fletcher et al., 1996)

DISCUSSION

Voltage sensor defect associated with tg^{rol} mutation

We have presented evidence that the tg^{rol} mutation causes a defect in the voltage-sensing mechanism of the P/Q-type Ca^{2+} channels. The nucleotide sequence alteration in the tg^{rol} mouse strain leads to the charge-neutralizing R-to-G substitution at the amino acid position 1262 in S4, which has been implicated as a voltage sensor of different voltage-gated channels (Stühmer et al., 1989; Liman et al., 1991; Papazian et al., 1991; Garcia et al., 1997), of repeat III in the P/Q-type α_{1A} subunit. Interestingly, this residue is conserved throughout Ca^{2+} channel α_1 subunits and Na^+ channel α subunits, suggesting a universal and essential role of the arginine residue in the operation of S4 as the voltage sensor. Both the recombinant α_{1A} channel with the tg^{rol} mutation and the native P-type channels in Purkinje cells acutely dissociated from tg^{rol} mouse cerebella showed similar modified voltage dependence of activation: midpoint potential was shifted to the depolarizing direction, and the steepness of activation curve was decreased. This is supported by slope factors (k_a) obtained through limiting slope analysis. The valence of the apparent single-gate charge for activation (z_m) calculated from the k_a value, using the equation $z_m = kT/k_a e_0 = 25.7/k_a$, was reduced from 4.2 to 3.2 by the mutation in the recombinant α_{1A} channel and from 5.0 to 4.0 in the native P-type channel (Hille, 1992). The decrease in z_m is 1.0 and is exactly what one would predict if the positively charged guanidino group of R1262 constitutes the gating charge that senses membrane depolarization.

Important human genetic diseases are associated with mutations that induce amino acid change in the voltage-sensing region of voltage-dependent channels. Point mutations of an autosomal dominant skeletal muscle disorder, hypokalemic periodic paralysis (hypo-KPP), predict R-to-H (histidine) substitutions in repeat II S4 and repeat IV S4 of the skeletal muscle α_{1S} isoform (Jurkat-Rott et al., 1994; Ptácek et al., 1994; Ophoff et al., 1996), whereas one of the familial hemiplegic migraine (FHM) mutations causes an R-to-Q (glutamine) amino acid substitution in repeat I S4 of the P/Q-type α_{1A} subunit (Ophoff et al., 1996). The mutations caused no significant alteration in voltage dependence of activation but rather reduced Ca^{2+} channel current density (Sipos et al., 1995; Lerche et al., 1996; Kraus et al., 1998; Hans et al., 1999). This is inconsistent with the theoretically predicted role of the charged residues that constitute gating charge of the voltage sensor S4 (see above). A recent report using the C terminus-truncated α_{1A} channel demonstrated that only little change in the slope factor of conductance–voltage curve was induced by the two hypo-KPP S4 mutations (Moril and Cannon, 1999). Furthermore, Long-QT syndrome LQT3 mutations that lead to the sporadic R-to-Q and heritable R-to-H substitutions in IVS4 of the cardiac SCN5A Na^+ channel are associated with delayed inactivation, but not with alteration in voltage dependence of activation (Wang et al., 1995; Wang et al., 1996; Kambouris et al., 1998; Makita et al., 1998). In LQT2, positive charge-neutralizing R-to-cysteine (C) substitution (R534C) in Herg K^+ channel S4 steepened the slope of activation curve, which can be theoretically expected for addition of gating charge to the voltage sensor S4 (Nakajima et al., 1999). Thus, among various spontaneous mutations of voltage-gated channels, tg^{rol} may so far represent the only mutation that produces the defect of the so-called "gating charge" of the voltage sensor (Hille, 1992).

Our results suggest that R1262 is also involved in inactivation mechanism of Ca^{2+} channels, in accordance with the idea that voltage-dependent activation and inactivation are coupled mechanisms. Interestingly, the effect of tg^{rol} R1262G substitution on voltage dependence of inactivation was only seen in native systems. It is therefore possible that the role of R1262 in inactivation is elicited only in the P-type splice variant of the α_{1A} subunit or in the presence of β_4 in Purkinje cells but not β_{1a} coexpressed in the recombinant system.

Impaired action potential generation in tg^{rol} Purkinje neurons

Our experiments demonstrate that whereas Na^+-dependent action potentials can be generated by weak depolarizations in the tg^{rol} mutant mice, large depolarizing currents caused depolarization of the membrane potential and termination of action potentials. Similar depolarization block was observed in normal Purkinje cells when the Ca^{2+} channels were blocked with Cd^{2+}, suggesting involvement of Ca^{2+}-activated K^+ channels (Llinás and Sugimori, 1980; Raman and Bean, 1999). In fact, Ca^{2+}-activated K^+ chan-

nels are known to be present in both the somatic and dendritic regions and play an important role in spike repolarization (Gruol et al., 1991). Taken together, one of the consequences of the tg^{rol} mutation is that reduced Ca^{2+} influx in tg^{rol} Purkinje neurons fails to activate the Ca^{2+}-activated K^+ channels, leading to depolarization block of Na^+ spikes. The possibility, however, that the density or localization of Na^+ channels is altered from secondary effects of the mutation via gene regulation or development, which results in the abortive Na^+ spike bursts, cannot be excluded.

When a large depolarizing current was injected for a prolonged duration, normal Purkinje neurons showed Ca^{2+} spikes, followed by bursts of Na^+ action potentials (Llinás and Sugimori, 1980). By contrast, Ca^{2+} spikes were hardly evoked in the mutant mice, and even when the Ca^{2+} spikes were generated, bursts of Na^+ spikes were not observed. This is presumably attributable to the direct consequence of the tg^{rol} mutation altering the voltage dependence of the P-type channels in Purkinje cells. A large depolarizing current that is capable of activating tg^{rol} Ca^{2+} channels may inactivate the Na^+ channels, or very long depolarization may cause slowly developing inactivation of the Na^+ channels.

Purkinje cells shows spatial segregation of the voltage-dependent Na^+ and Ca^{2+} conductances. Whereas the voltage-dependent Na^+ channels are restricted to the soma and axon, the voltage-dependent Ca^{2+} channels are mainly distributed in dendrites, being capable of generating dendritic Ca^{2+} spikes (Llinás and Sugimori, 1980). Because Ca^{2+} spikes in the dendritic tree play an essential role in integration of synaptic inputs, compromised Ca^{2+} spike generation in the tg^{rol} mice would severely impair function of the cerebellum.

Altered P-type channel function and neurological phenotypes

Cerebellar ataxia has been identified as a common behavioral abnormality among the three α_{1A} mutant mice tg^{rol}, tg^{la}, and tg. However, severity of cerebellar ataxia differs significantly among tg^{rol}, tg^{la}, and tg mice; severity of ataxia of tg^{rol} falls somewhere in between those of tg^{la} and tg. tg^{la} and tg^{rol} suffer from loss/degeneration of cerebellar neurons (Nishimura, 1975; Herrup and Wilczynski, 1982). The present data on tg^{rol} mice in combination with our previous work on tg^{la} and tg mice (Wakamori et al., 1998) suggest that severity of the cerebellar defect in the mutant strains is somewhat correlated with deviation of P-type channel properties in Purkinje cells. Reduction in P-type Ca^{2+} current amplitude was the severest in tg^{la} Purkinje cells (~60%) compared with those in tg and tg^{rol} cells (~40%). Voltage dependence of activation of tg^{la} and tg^{rol} P-type channels but not that of tg P-type channels showed depolarizing shift. P-type currents in the tg^{rol} and tg^{la} mutant displayed shift of voltage dependence of inactivation, whereas decrease in fraction of inactivation during 2 sec depolarization was observed for the tg^{la} and tg P-type currents. In the null mutant mice lacking the expression of the α_{1A} subunit, a complete loss of P-type channel function induces an ataxia that progressively worsened up to the point of premature death (Jun et al., 1999). It is thus possible that intermediate severity of ataxia in tg^{rol} mice reflects intermediate deviation of P-type channel function, which results in corresponding impairment of integrative properties of Purkinje cells in motor function.

Additional neurological differences are seen among the three P/Q-type α_{1A} subunit mutants. tg^{la} and tg mice display absence epilepsy (Noebels, 1984), but tg^{rol} mice do not (Oda, 1981). Only tg mice suffer from paroxysmal dyskinesis (Green and Sidman, 1962). The differences may derive from different involvement of the P/Q-type channel activity in respective neuronal functions. Because apoptosis has been observed only in tg^{la} cerebella, which contain the most severely functionally impaired P/Q-type channels, P/Q-type channels may exert redundant activity in increasing the intracellular Ca^{2+} concentration required for cell survival (Yano et al., 1998). By contrast, TH expression, which is ectopic in the cerebella of the three mutants, should be tightly regulated by P/Q-type channel activity. It is, however, difficult to discuss the genesis of absence seizures in the similar context, because experimental studies and clinical observations indicate a central role of thalamocortical circuits that comprise multiple neuronal populations. Furthermore, absence epilepsy can be generated as a consequence of prolonged and inappropriate expression of developmentally immature complexation between the N-type α_{1B} subunit and β subunit isoforms (McEnery et al., 1998). As a matter of fact, tg^{rol} mice in which impairment of P/Q-type channel function is intermediate do not show apparent absence seizures. Future work using slice preparation together with intracellular Ca^{2+} concentration measurements should allow us to more precisely and qualitatively correlate the P/Q-type channel function with respective cellular functions. In this regard, *Rocker* (tg^{rok}) mutant that shows interesting phenotypes such as degeneration of axon, reduction of branching in the Purkinje cell dendritic arbor, and a "weeping willow" appearance of the secondary branches, should provide us with an avenue in understanding the contribution of the P/Q-type channel in development and morphogenesis of dendritic trees in Purkinje cells (Zwingman et al., 1997, 1999).

REFERENCES

Ahlijanian MK, Westenbroek RE, Catterall WA (1990) Subunit structure and localization of dihydropyridine-sensitive calcium channels in mammalian brain, spinal cord, and retina. Neuron 4:819–832.

Artalejo CR, Adams ME, Fox AP (1994) Three types of Ca^{2+} channel trigger secretion with different efficacies in chromaffin cells. Nature 367:72–76.

Bean BP (1989) Classes of calcium channels in vertebrate cells. Annu Rev Physiol 51:367–384.

Bourinet E, Soong TW, Sutton K, Slaymaker S, Mathews E, Monteil A, Zamponi GW, Nargeot J, Snutch TP (1999) Splicing of α_{1A} subunit gene generates phenotypic variants of P- and Q-type calcium channels. Nat Neurosci 2:407–415.

Campbell KP, Leung AT, Sharp AH (1988) The biochemistry and molecular biology of the dihydropyridine-sensitive calcium channel. Trends Neurosci 11:425–430.

Chen C, Okayama H (1987) High-efficiency transformation of mammalian cells by plasmid DNA. Mol Cell Biol 7:2745–2752.

Clapham DE (1995) Calcium signaling. Cell 80:259–268.

Dove LS, Abbott LC, Griffith WH (1998) Whole-cell and single-channel analysis of P-type calcium currents in cerebellar Purkinje cells of leaner mutant mice. J Neurosci 18:7687–7699.

Fletcher CF, Lutz CM, O'Sullivan TN, Shaughnessy Jr JD, Hawkes R, Frankel WN, Copeland NG, Jenkins NA (1996) Absence epilepsy in tottering mutant mice is associated with calcium channel defects. Cell 87:607–617.

Fujita Y, Mynlieff M, Dirksen RT, Kim M-S, Niidome T, Nakai J, Friedrich T, Iwabe N, Miyata T, Furuichi T, Furutama D, Mikoshiba K, Mori Y, Beam KG (1993) Primary structure and functional expression of the ω-conotoxin-sensitive N-type calcium channel from rabbit brain. Neuron 10:585–598.

Garcia J, Nakai J, Imoto K, Beam KG (1997) Role of S4 segments and the leucine heptad motif in the activation of an L-type calcium channel. Biophys J 72:2515–2523.

Glossmann H, Striessnig J (1990) Molecular properties of calcium channels. Rev Physiol Biochem Pharmacol 114:1–105.

Green MC, Sidman RL (1962) Tottering: a neuromuscular mutation in the mouse. J Hered 53:79–94.

Gruol DL, Jacquin T, Yool AJ (1991) Single-channel K^+ currents recorded from the somatic and dendritic regions of cerebellar Purkinje neurons in culture. J Neurosci 11:1002–1015.

Hamill OP, Marty A, Neher E, Sakmann B, Sigworth FJ (1981) Improved patch-clamp techniques for high-resolution current recording from cells and cell-free membrane patches. Pflügers Arch 391:85–100.

Hans M, Luvisetto S, Williams ME, Spagnolo M, Urrutia A, Tottene A, Brust PF, Johnson EC, Harpold MM, Stauderman KA, Pietrobon D (1999) Functional consequences of mutations in the human α_{1A} calcium channel subunit linked to familial hemiplegic migraine. J Neurosci 19:1610–1619.

Herrup K, Wilczynski SL (1982) Cerebellar cell degeneration in the leaner mutant mouse. Neuroscience 7:2185–2196.

Hess EJ, Wilson MC (1991) Tottering and leaner mutations perturb transient developmental expression of tyrosine hydroxylase in embryologically distinct Purkinje cells. Neuron 6: 123–132.

Hille B (1992) Ionic channels of excitable membranes, Ed 2. Sunderland, MA: Sinauer.

Hirning LD, Fox AP, McCleskey EW, Olivera BM, Thayer SA, Miller RJ, Tsien RW (1988) Dominant role of N-type Ca^{2+} channels in evoked release of norepinephrine from sympathetic neurons. Science 239:57–61.

Jun K, Piedras-Renteria ES, Smith SM, Wheeler DB, Lee SB, Lee TG, Chin H, Adams ME, Scheller RH, Tsien RW, Shin HS (1999) Ablation of P/Q-type Ca^{2+} channel currents, altered synaptic transmission, and

progressive ataxia in mice lacking the α_{1A}-subunit. Proc Natl Acad Sci USA 96:15245–15250.
Jurkat-Rott K, Lehmann-Horn F, Elbaz A, Heine R, Gregg RG, Hogan K, Powers PA, Lapie P, Vale-Santos JE, Weissenbach J, Fontaine B (1994) A calcium channel mutation causing hypokalemic periodic paralysis. Hum Mol Genet 3:1415–1419.
Jurman ME, Boland LM, Liu Y, Yellen G (1994) Visual identification of individual transfected cells for electrophysiology using antibody-coated beads. BioTechniques 17:876–881.
Kambouris NG, Nuss HB, Johns DC, Tomaselli GF, Marban E, Balser JR (1998) Phenotypic characterization of a novel long-QT syndrome mutation (R1623Q) in the cardiac sodium channel. Circulation 97:640–644.
Klöckner U, Mikala G, Varadi M, Varadi G, Schwartz A (1995) Involvement of the carboxyl-terminal region of the α_{1A} subunit in voltage-dependent inactivation of cardiac calcium channels. J Biol Chem 270:17306–17310.
Kobayashi T, Mori Y (1998) Ca^{2+} channel antagonists and neuroprotection from cerebral ischemia. Eur J Pharmacol 363:1–15.
Kraus RL, Sinnegger MJ, Glossmann H, Hering S, Striessnig J (1998) Familial hemiplegic migraine mutations change α_{1A} Ca^{2+} channel kinetics. J Biol Chem 273:5586–5590.
Lee JH, Daud AN, Cribbs LL, Lacerda AE, Pereverzev A, Klöckner U, Schneider T, Perez-Reyes E (1999) Cloning and expression of a novel member of the low voltage-activated T-type calcium channel family. J Neurosci 19:1912–1921.
Lerche H, Klugbauer N, Lehmann-Horn F, Hofmann F, Melzer W (1996) Expression and functional characterization of the cardiac L-type calcium channel carrying a skeletal muscle DHP-receptor mutation causing hypokalaemic periodic paralysis. Pflügers Arch 431:461–463.
Letts VA, Felix R, Biddlecome GH, Arikkath J, Mahaffey CL, Valenzuela A, Bartlett II FS, Mori Y, Campbell KP, Frankel WN (1998) The mouse stargazer gene encodes a neuronal Ca^{2+}-channel γ subunit. Nat Genet 19:340–347.
Liman ER, Hess P, Weaver F, Koren G (1991) Voltage-sensing residues in the S4 region of a mammalian K^+ channel. Nature 353:752–756.
Llinás R, Sugimori M (1980) Electrophisiological properties of in vitro Purkinje cell somata in mammalian cerebellar slices. J Physiol (Lond) 305:171–195.
Llinás R, Sugimori M, Lin JW, Cherksey B (1989) Blocking and isolation of a calcium channel from neurons in mammals and cephalopods utilizing a toxin fraction (FTX) from funnel-web spider poison. Proc Natl Acad Sci USA 86:1689–1693.
Llinás R, Sugimori M, Hillman DE, Cherksey B (1992) Distribution and functional significance of the P-type, voltage-dependent Ca^{2+} channels in the mammalian central nervous system. Trends Neurosci 15:351–355.
Lorenzon NM, Lutz CM, Frankel WN, Beam KG (1998) Altered calcium channel currents in Purkinje cells of the neurological mutant mouse *leaner*. J Neurosci 18:4482–4489.
Makita N, Shirai N, Nagashima M, Matsuoka R, Yamada Y, Tohse N, Kitabatake A (1998) A *de novo* missense mutation of human cardiac Na^+ channel exhibiting novel molecular mechanisms of long QT syndrome. FEBS Lett 423:5–9.
Matsuyama Z, Wakamori M, Mori Y, Kawakami H, Nakamura S, Imoto K (1999) Direct alteration of the P/Q-type Ca^{2+} channel property by polyglutamine expansion in spinocerebellar ataxia 6. J Neurosci 19:RC14 (1–5).
McEnery MW, Copeland TD, Vance CL (1998) Altered expression and assembly of N-type calcium channel α_{1B} and β subunits in epileptic *lethargic* (*lh*/*lh*) mouse. J Biol Chem 273:21435–21438.
Mintz IM, Venema VJ, Swiderek KM, Lee TD, Bean BP, Adams ME (1992) P-type calcium channels blocked by the spider toxin ω-Aga-IVA Nature 355:827–829.
Mori Y, Friedrich T, Kim MS, Mikami A, Nakai J, Ruth P, Bosse E, Hofmann F, Flockerzi V, Furuichi T, Mikoshiba K, Imoto K, Tanabe T, Numa S (1991) Primary structure and functional expression from complementary DNA of a brain calcium channel. Nature 350:398–402.
Moril JA, Cannon SC (1999) Effects of mutations causing hypokalaemic periodic paralysis on the skeletal muscle L-type Ca^{2+} channel expressed in *Xenopus laevis* oocytes. J Physiol (Lond) 520:321–336.
Mukaiyama M, Mizuno K (1976) Cerebellum of rolling mouse Nagoya. Saishin Igaku 31:233–236.
Nakajima T, Furukawa T, Hirano Y, Tanaka T, Sakurada H, Takahashi T, Nagai R, Itoh T, Katayama Y, Nakamura Y, Hiraoka M (1999) Voltage-shift of the current activation in *HERG* S4 mutation (R534C) in LQT2. Cardiovascular Res 44:283–293.
Niidome T, Teramoto T, Murata Y, Tanaka I, Seto T, Sawada K, Mori Y, Katayama K (1994) Stable expression of the neuronal BI (Class A) calcium channel in the baby hamster kidney cells. Biochem Biophys Res Commun 203:1821–1827.
Nishimura Y (1975) The cerebellum of rolling mouse Nagoya. Adv Neurological Sci 19:670–672.
Noebels JL (1984) Isolating single genes of the inherited epilepsies. Ann Neurol 16:S18–21.
Oda S (1973) The observation of rolling mouse Nagoya (*rol*), a new neurological mutant and its maintenance. Exp Anim 22:281–288.
Oda S (1981)A new allele of the tottering locus, rolling mouse Nagoya, on chromosome no. 8 in the mouse. Jpn J Genet 56: 295–299.
Ophoff RA, Terwindt GM, Vergouwe MN, van Eijk R, Oefner PJ, Hoffman SM, Lamerdin JE, Mohrenweiser HW, Bulman DE, Ferrari M, Haan J, Lindhout D, van Ommen GJ, Hofker MH, Ferrari MD, Frants RR (1996) Familial hemiplegic migraine and episodic ataxia type-2 are caused by mutations in the Ca^{2+} channel gene CACNL1A4. Cell 87:543–552.
Papazian DM, Timpe LC, Jan YN, Jan LY (1991) Alteration of voltage-dependence of Shaker potassium channel by mutations in the S4 sequence. Nature 349:305–310.
Ptácek LJ, Tawil R, Griggs RC, Engel AG, Layzer RB, Kwiecinski H, McManis PG, Santiago L, Moore M, Fouad G, Bradley P, Leppert MF (1994) Dihydropyridine receptor mutations cause hypokalemic periodic paralysis. Cell 17:863–868.
Raman IM, Bean BP (1999) Ionic currents underlying spontaneous action potentials in isolated cerebellar Purkinje neurons. J Neurosci 19:1663–1674.
Regan LJ, Sah DW, Bean BP (1991) Ca^{2+} channels in rat central and peripheral neurons: high-threshold current resistant to dihydropyridine blockers and ω-conotoxin. Neuron 6:269–280.
Regehr WG, Mintz IM (1994) Participation of multiple calcium channel types in transmission at single climbing fiber to Purkinje cell synapses. Neuron 12:605–613.
Sather WA, Tanabe T, Zhang JF, Mori Y, Adams ME, Tsien RW (1993) Distinctive biophysical and pharmacological properties of class A (BI) calcium channel α_1 subunits. Neuron 11:291–303.
Sipos I, Jurkat-Rott K, Harasztosi C, Fontaine B, Kovacs L, Melzer W, Lehmann-Horn F (1995) Skeletal muscle DHP receptor mutations alter calcium currents in human hypokalaemic periodic paralysis myotubes. J Physiol (Lond) 483:299–306.
Stea A, Tomlinson WJ, Soong TW, Bourinet E, Dubel SJ, Vincent SR, Snutch TP (1994) Localization and functional properties of a rat brain α_{1A} calcium channel reflect similarities to neuronal Q- and P-type channels. Proc Natl Acad Sci USA 91:10576–10580.
Stühmer W, Conti F, Suzuki H, Wang XD, Noda M, Yahagi N, Kubo H, Numa S (1989) Structural parts involved in activation and inactivation of the sodium channel. Nature 339:597–603.
Takahashi T, Momiyama A (1993) Different types of calcium channels mediate central synaptic transmission. Nature 366:156–158.
Tsien RW, Ellinor PT, Horne WA (1991) Molecular diversity of voltage-dependent Ca^{2+} channels. Trends Pharmacol Sci 12:349–354.
Turner TJ, Adams ME, Dunlap K (1992) Calcium channels coupled to glutamate release identified by ω-Aga-IVA Science 258: 310–313.
Wakamori M, Hidaka H, Akaike N (1993) Hyperpolarizing muscarinic responses of freshly dissociated rat hippocampal CA1 neurones. J Physiol (Lond) 463:585–604.
Wakamori M, Yamazaki K, Matsunodaira H, Teramoto T, Tanaka I, Niidome T, Sawada K, Nishizawa Y, Sekiguchi N, Mori E, Mori Y, Imoto K (1998) Single tottering mutations responsible for the neuropathic phenotype of the P-type calcium channel. J Biol Chem 273:34857–34867.
Wang DW, Yazawa K, George AL Jr, Bennett PB (1996) Characterization of human cardiac Na^+ channel mutations in the congenital long QT syndrome. Proc Natl Acad Sci USA 93:13200–13205.
Wang Q, Shen J, Splawski I, Atkinson D, Li Z, Robinson JL, Moss AJ, Towbin JA, Keating MT (1995) SCN5A mutations associated with an inherited cardiac arrhythmia, long QT syndrome. Cell 80:805–811.
Witcher DR, De Waard M, Sakamoto J, Franzini-Armstrong C, Pragnell M, Kahl SD, Campbell KP (1993) Subunit identification and reconstitution of the N-type Ca^{2+} channel complex purified from brain. Science 261:486–489.
Yano S, Tokumitsu H, Soderling TR (1998) Calcium promotes cell survival through CaM-K kinase activation of the protein-kinase-B pathway. Nature 396:584–587.
Zhang J-F, Randall AD, Ellinor PT, Horne WA, Sather WA, Tanabe T, Schwarz TL, Tsien RW (1993) Distinctive pharmacology and kinetics of cloned neuronal Ca^{2+} channels and their possible counterparts in mammalian CNS neurons. Neuropharmacology 32:1075–1088.
Zhuchenko O, Bailey J, Bonnen P, Ashizawa T, Stockton DW, Amos C, Dobyns WB, Subramony SH, Zoghbi HY, Lee CC (1997) Autosomal dominant cerebellar ataxia (SCA6) associated with small polyglutamine expansions in the α_{1A}-voltage-dependent calcium channel. Nat Genet 15:62–69.
Zwingman TA, Neumann PE, Herrup K (1997) Characterization of Rocker, a novel ataxic mouse mutant. Soc Neurosci Abstr 23:605.
Zwingman TA, Neumann PE, Noebels JL, Herrup K (1999) Rocker, a new allele of tottering. Soc Neurosci Abstr 25:722.